Study of Hybrid Excited Synchronous Alternators for Automotive Applications Using Coupled FE and Circuit Simulations

Thomas Finken and Kay Hameyer

Institute of Electrical Machines, RWTH Aachen University, D-52056 Aachen Germany

In this paper, an alternative arrangement to conventional Lundell automotive generators is examined. This geometry is characterized by hybrid excitation combining the high-energy density of permanent magnets and the controllability of commonly used electrical excitation. The rotor geometry of the alternator is optimized by means of finite element (FE) simulations and a prototype design is developed. The formulation for the transient solver is given and the coupling of the FE model with an external circuit is explained in detail. The accomplished studies, simulations, and geometry optimizations are presented. In a final step, the simulations are compared to prototype measurements and confronted with conventional alternator geometries.

Index Terms—**Hybrid excited, synchronous alternator.**

I. Introduction

AUTOMOTIVE power supply systems required for powering electrical equipment onboard and loading the battery contain an alternator. Due to the increase of electrical power consumption in modern vehicles, the efficiency of those alternators must be improved holding weight and volume constant, or even reducing them. Limited perspectives of improvement of existing alternator types leads to consideration of innovative concepts. The concept proposed in this paper is based on a hybrid rotor with both magnetic (PM) and electric (windings) excitation. Electric excitation offers an easier control of the magnetic field by controlling the excitation current, but yields a more complicated rotor construction and increased copper expenses. With new magnetic materials characterized by higher energy densities, improved temperature stability, and reasonable prices, the application of permanent-magnet excitation becomes more attractive and promises higher power densities. PM excitation on the other hand does not allow flux weakening, which has prevented it from being used in automotive applications in the past. Hence, the concept of hybrid excitation makes it possible to benefit at the same time from the high-energy density of PM and the controllability of electrical excitation [1].

II. Studied Geometry

The rotor under study consists of four permanent magnets and four electromagnets (windings) arranged alternately and symmetrically as depicted in Fig. 1. All magnets are magnetized in radial direction with all north poles oriented towards the air gap. Used permanent magnets are rare-earth magnets of NeFeB grades.

When the electromagnets are magnetized in the same direction as the permanent magnets, a symmetric 16 pole configuration is obtained, whose south poles are the return fluxes of the eight active north poles, as shown in Fig. 1. Induced voltage and delivered power are maximal in this case. With no electrical excitation now, an asymmetrical eight pole configuration is obtained, which due to the asymmetry still induces a nonzero voltage in the 16 pole stator coil arrangement. For a given negative excitation finally, the eight pole configuration becomes symmetric and the in voltage induced in stator windings is nearly zero, as well as the power delivered by the alternator.

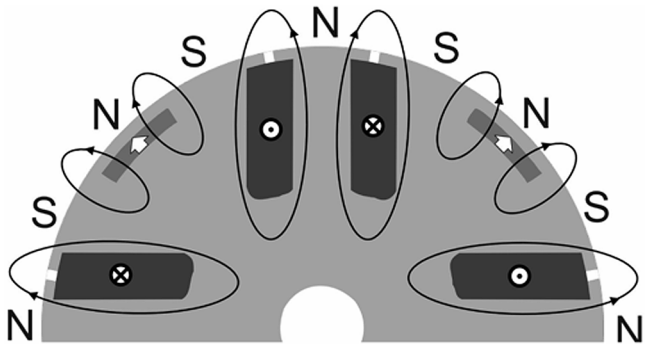

Fig. 1. Schematic geometry sector of examined rotor.

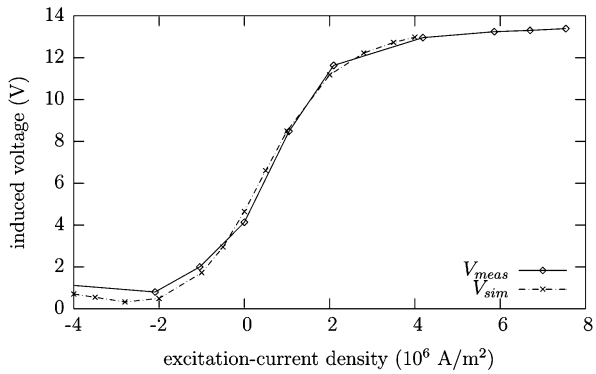

Fig. 2. Induced voltage versus excitation current at $n = 1000$ r/min.

This behavior is illustrated in Fig. 2, where the simulated and measured induced voltage are plotted versus the excitation-current density. In this study, the speed of the machine is kept constant at 1000 r/min. Without excitation current, the induced voltage is approximately 5 V. By increasing the excitation current, the induced voltage is increased linearly until the characteristics flatten due to the ferro–magnetic saturation. By decreasing now the excitation current in the opposite direction, the induced voltage decreases until the eight-pole rotor field is reached. In this case, the induced voltage has its minimum value.

Digital Object Identifier 10.1109/TMAG.2007.916114

III. Applied Transient Solver

To simulate the alternator in chosen operation points requires a transient solving process which takes the geometry rotation into account and is coupled to an electric circuit. The applied inhouse solver is part of an object-oriented solver package [2]. The transient finite element method (FEM) formulation takes rotation into account by means of time stepping, so two finite element (FE) meshes have to be handled at each time step. The 2-D $\vec{A}$ approach, using the magnetic vector potential $\vec{A}$ in all regions, has to be solved in the complete model Ω. Its Galerkin formulation is [2]

$$\int_\Omega \left(\operatorname{grad}\alpha_i \cdot \nu \operatorname{grad} A_z(t) + \alpha_i \cdot \frac{d}{dt}\sigma A_z(t)\right) d\Omega = \int_\Omega (\alpha_i \cdot J_z(t) + \operatorname{rot}(\alpha_i \vec{e}_z) \cdot \nu \vec{B}_r) d\Omega. \quad (1)$$

The material parameters ν and σ represent the nonlinear reluctivity and the linear conductivity. The nodal shape functions are denoted by α_i.$J_z(t)$ describes the z-component of the given coil-current density while $B_r(t)$ defines remanence of PM.

In the case of unknown stator currents, the electromagnetic computation has to be coupled with an electrical circuit. The magnetic vector potential $\vec{A}$ is still an unknown quantity of the system of equations. Furthermore, two kinds of electric conductors are distinguished: the solid conductor with possible eddy currents and the stranded conductor where, due to its thin wires, no eddy currents are possible. The unknown quantities are voltages for solid conductors and currents for stranded conductors. The magnetic vector potential $\mathbf{A}$, the voltage $\Delta\mathbf{V}$ of solid conductors, and the circuit-mesh current $\mathbf{I}_m$ make up the unknown vectors. The system matrices describing this FE approach are

$$\begin{bmatrix} \Theta\mathbf{S} + \frac{1}{\Delta t}\mathbf{G} & -\Theta\mathbf{C} & -\Theta\mathbf{C}'\mathbf{D}'^T \\ -\Theta\mathbf{C}^T & \Delta t\Theta^2 \frac{1}{\mathbf{R}} & -\Delta t\Theta^2\mathbf{D}^T \\ -\Theta\mathbf{D}'\mathbf{C}'^T & -\Delta t\Theta^2\mathbf{D} & -\Theta\mathbf{L}_m - \Delta t\Theta^2\mathbf{R}'_m \end{bmatrix}\Bigg|_{n+1} \cdot \begin{bmatrix} A_{n+1} \\ \Delta V_{n+1} \\ I_{m_{n+1}} \end{bmatrix} = \begin{bmatrix} -(1-\Theta)\mathbf{S} + \frac{1}{\Delta t}\mathbf{G} & (1-\Theta)\mathbf{C} & (1-\Theta)\mathbf{C}'\mathbf{D}'^T \\ -\Theta\mathbf{C}^T & -\Delta t\Theta(1-\Theta)\frac{1}{\mathbf{R}} & \Delta t\Theta(1-\Theta)\mathbf{D}^T \\ -\Theta\mathbf{D}'\mathbf{C}'^T & \Delta t\Theta(1-\Theta)\mathbf{D} & -\Theta\mathbf{L}_m - \Delta t\Theta(1-\Theta)\mathbf{R}'_m \end{bmatrix} \cdot \begin{bmatrix} A_n \\ \Delta V_n \\ I_{m_n} \end{bmatrix} + \begin{bmatrix} 0 \\ 0 \\ -\Delta t\Theta^2 U_{m_{n+1}} - \Delta t\Theta(1-\Theta)U_{m_n} \end{bmatrix}. \quad (2)$$

Whereas the element matrices $\mathbf{G}, \mathbf{C}$, and $\mathbf{R}_k$ describe the solid conductor regions, $\mathbf{G}'$, $\mathbf{C}'$, and $\mathbf{R}'_k$ describe stranded conductor regions. In case of coupled circuit simulation and considered rotational movement, the element matrix $\mathbf{S}$ is

$$S_{ij}|_{n+1} = l\int_F \operatorname{grad}\alpha_{i_{n+1}} \cdot \nu_{n+1} \operatorname{grad}\alpha_{j_{n+1}} dF \quad (3)$$

$$S_{ij}|_n = l\int_F \operatorname{grad}\alpha_{i_n} \cdot \nu_n \operatorname{grad}\alpha_{j_n} dF. \quad (4)$$

For the simulation, the defined slot conductors of the FE model were coupled with star- or delta-connected external circuits. A star-connected ohmic load was included to simulate

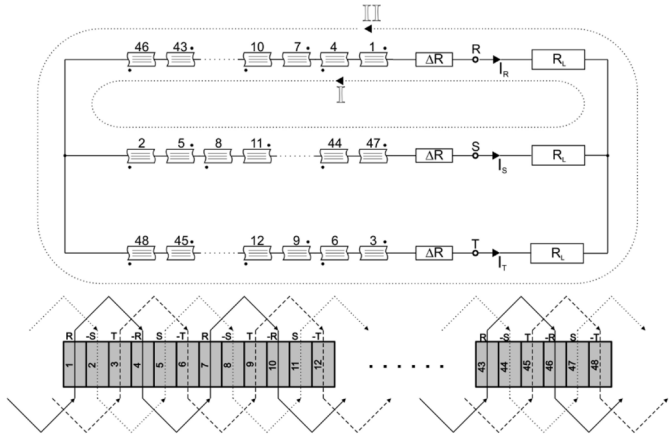

Fig. 3. Star-connected alternator with ohmic load.

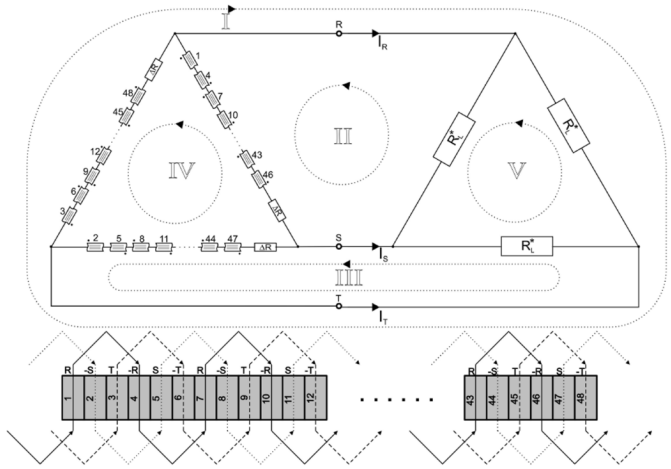

Fig. 4. Delta-connected alternator with ohmic load.

several operation points. To compare geometry variations, the optimization steps, and the hybrid concept with conventional alternators, three load states versus the rotational speed were examined: the voltage in no-load operation, the current in short-circuit operation, and the delivered power with a load of 1Ω star connected resistors.

The star connected alternator and the interconnection of the coil-material labels are shown in Fig. 3. The component R_L represents the ohmic load. The additional resistor and inductances of the end windings are considered with the components ΔR. Due to convergence difficulty, the star-connected ohmic load has to be converted into an equivalent delta connected ohmic load in the case of the delta connected alternator (Fig. 4).

To verify the calculated results, they were compared to measured values and sufficient conformity was determined. Exemplarily, the evaluation and comparison of voltages induced in star- and delta-connected alternator is presented. Due to third harmonics of the excitation field, voltages are induced in the stator coils, which are not 120° phase shifted, but in phase. Currents result from these voltages if the alternator is delta connected. These ring currents, just limited by relative small coil resistances, can reach high values, thus they counteract the third harmonics of the excitation field and nearly erase them. The resulted difference between the voltages as well as the conformity

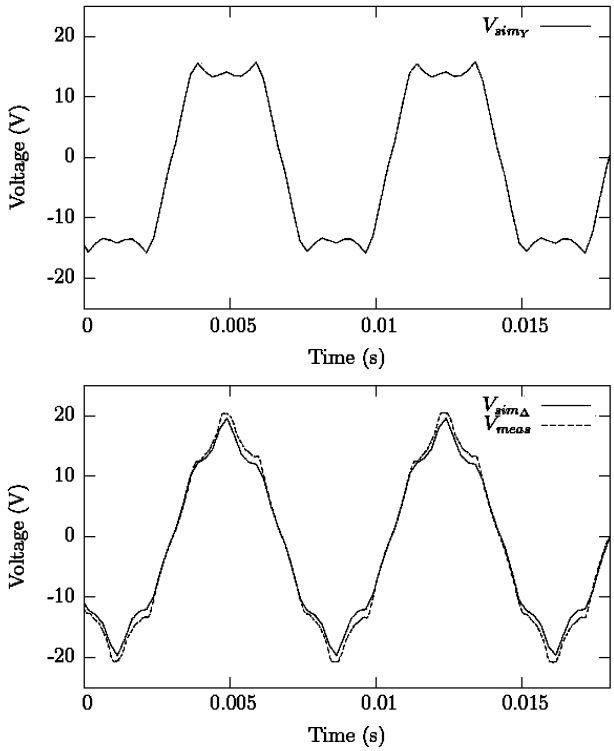

Fig. 5. Voltage of star- and delta-connected alternator.

with measured values is illustrated in Fig. 5. Furthermore the simulated currents in load operation and short-circuit operation were compared to measured values of the prototype.

IV. Results and Accomplished Studies

The rotor geometry was optimized with respect to various considerations. The embedding of the permanent magnets, the pole arc, and the geometry of the excitation-winding slots was studied as well as the assembly of more than one permanent magnet per pole. Additionally the influence of pole chamfer was examined in regard to later acoustic noise optimization of the generator. Two of these studies are presented in the next section.

A. Design of the Embedded Permanent Magnets

Automotive alternators are tightly coupled to the combustion engine, commonly with a 1 : 3 gear ratio, so the rotor may be operated at speeds up to 18 000 r/min, causing considerable material stress. For this reason, the permanent magnets are buried. However, there is a disadvantage. Because magnets are entirely surrounded by ferromagnetic steel, the main part of the magnetic flux may close in the rotor—a magnetic short circuit. This flux neither crosses the air gap nor the stator coils and it is not available for voltage induction. The flux linkage is approximately 44% [Fig. 6(a)].

By making flux barriers (notches near the magnets) at the outer rotor radius, the area, available for magnetic short-circuit, can be reduced. As the saturation of this area increases, the magnetic resistance via air gap and stator will relatively decrease and a larger part of the magnetic flux will accordingly close through air gap and rotor. However, the remaining permanent-magnet support must assure sufficient mechanical fixation at high speed.

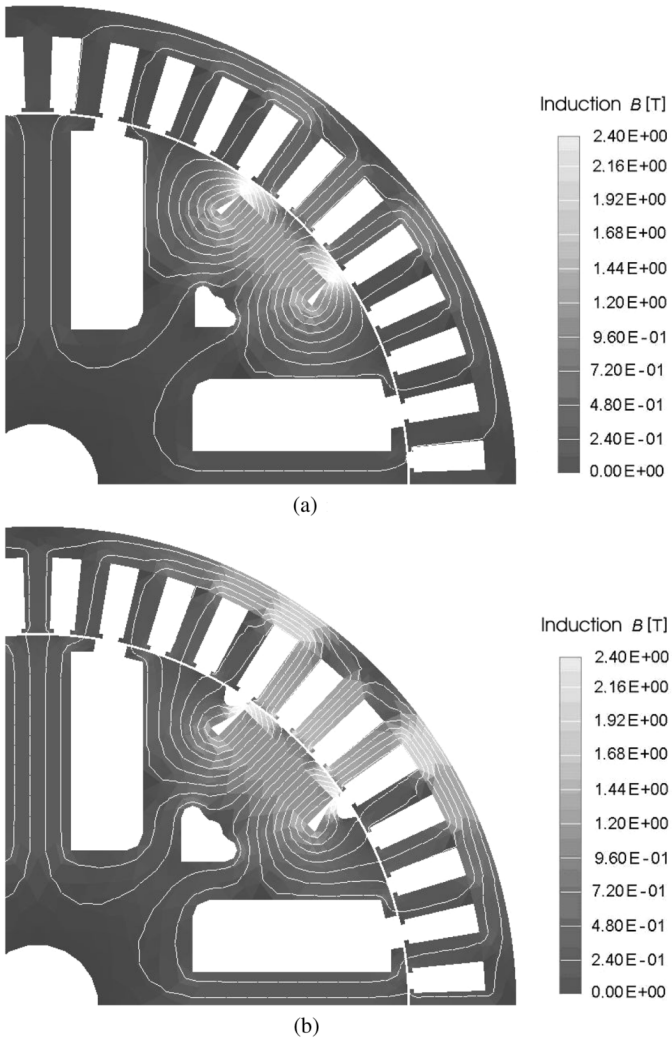

Fig. 6. Magnetic field depending on flux concentration. (a) No flux concentration. (b) Geometry with notches and increased PM height.

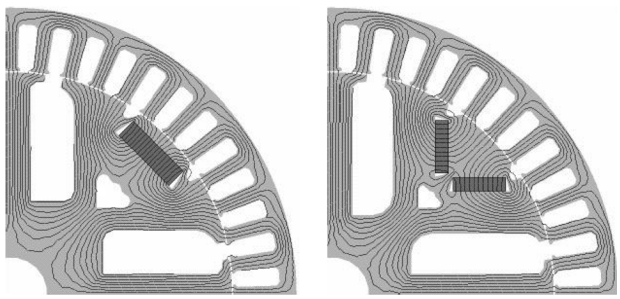

Fig. 7. Geometries with one and two permanent magnets per pole.

A compromise between sufficient fixation and efficient permanent-magnet use has to be found. Fig. 6(b) shows the last step of the development in which the flux linkage was increased up to 75%, maintaining a sufficient strength of the magnet support.

B. Design With Two Permanent Magnets Per Pole

Instead of one magnet per permanent-magnet excited pole, two magnets can be used in a v-form arrangement (Fig. 7). This arrangement increases the available magnet area and permits a

TABLE I
SIMULATED VALUES OF DELIVERED POWER

	delivered power (W)		
	1000rpm	3000rpm	6000rpm
K16	155	1019	4999
K16-W	161	1328	5046
K16-2PM	159	1404	5334
SPSG	88	788	2998
Lundell	147	1323	5043

higher magnetic flux. However, it also requires an adjustment close to the excitation windings due to the early occurrence of saturation between the winding and the magnet. For this reason, the coil areas are designed narrower. To keep the size of the area, the coil areas are extended by the same factor. Two attempts were examined in this work: first, to reach the same usable flux with fewer permanent-magnet material and second, to reach an increased output power with constant magnet material.

In the first case, a design was found that reaches the same flux with only half of the PM material. A comparison of the simulation results shows the same induced voltage, but decreased maximum current (about 7%). In the second case, the area of the single permanent magnet was divided into two magnets. With this arrangement, a flux linkage 8% higher than the previous one was obtained. Due to the larger usable flux linkage, the induced voltage increases about 5% and the maximum current increases about 12.4%. Depending on the speed, there are power gains of up to 13%. Performed studies show that it is possible either to save permanent-magnet material or to generate a higher output power with the same material quantity—production expense of inserting the magnets would nearly be constant. However, it has to be considered that, due to the higher magnetic flux, the already high cogging torque will increase further.

C. Comparison of Rotor Types

To ensure a good comparability, the simulations of all rotor types were accomplished with the same number of poles and identical stator geometry and external circuit, respectively. This stator was part of a Lundell-type alternator and was also used for prototyping the studied hybrid machine design.

In Table I, the simulated delivered output power is presented at particular rotor speeds. Compared geometries are the studied design (K16), a salient pole synchronous machine (SPSG), and the Lundell-type alternator. Presented versions of the K16 design are the design used for prototyping and two further developments: one with improved geometry with respect to magnetic saturation (K16-W) and the other design featuring two magnets per pole (K16-2PM). The final rotor geometry (K16-2PM) delivered about 5% more electrical power compared to Lundell alternator with identical stator.

TABLE II
POWER DENSITY OF COMPARED GEOMETRIES

	power (W)	weight (g)	power/weight (W/kg)
K16	4999	4335	1153
K16-W	5046	4333	1165
K16-2PM	5334	4362	1223
SPSG	2998	4456	673
Lundell	5043	4781	1055

Comparing the weights of the different rotor geometries indicates that the studied rotor was about 15% lighter in weight. This is due to its axial length—in contrast to the Lundell type where the rotor length is more than twice the stator length. The weights collected in Table II are the weights of the active machine components such as stator, rotor, and windings. Other components like casing are neglected, because they are the same for all studied rotor geometries as mentioned before. Due to the lower weight and higher power, the power density of the studied geometry is increased by about 14%.

V. CONCLUSION

Comparison with measurements on built prototype showed that the applied transient FE simulation coupled with external circuit is suitable to simulate electrical machines in generator mode. By that means it was possible to study, optimize, and compare the hybrid excited alternator concept to conventional alternator designs before prototyping. The optimized geometry delivers about 5% more power, but the weight was reduced by 15% compared to the Lundell generator.

REFERENCES

[1] L. Zhenguang, X. Yanliang, T. Renyuan, and H. Yan, "3D magnetic field analysis of a hybrid excitation synchronous generator," in *IEEE Proc. 5th Int. Conf. Electr. Mach. Syst.*, 2001, vol. 1, pp. 164–166.

[2] D. van Riesen, C. Monzel, C. Kaehler, C. Schlensok, and G. Henneberger, "iMOOSE—An open-source environment for finite-element calculations," *IEEE Trans. Magn.*, vol. 40, no. 2, pp. 1390–1393, 2004.

[3] G. Arians and G. Henneberger, "Object oriented analysis and design of transient finite element solvers applied to coupled problems," in *Dig. 9th CEFC*, Milwaukee, WI, Jun. 2000, p. 449.

[4] F. B. Reiter, K. Rajashekara, and R. J. Krefta, "Salient pole generators for belt-driven automotive alternator applications," presented at the IEEE 36th IAS Annu. Meeting Ind. Appl. Conf., Chicago, IL, Sep. 30–Oct. 4 2001.

[5] P. Salminen, "Fractional slot permanent magnet synchronous motors for low speed application," Ph.D. dissertation, Lappeenranta Univ. Technol., Lappeenranta, Finland, 2004.

[6] F. Libert and J. Soulard, "Design study of different direct-driven permanent-magnet motors for a low speed application," presented at the IEEE 40th IAS Annu. Meeting Ind. Appl. Conf., Lausanne, Switzerland, Sep. 2005.

Manuscript received June 24, 2007. Corresponding author: T. Finken (e-mail: thomas.finken@iem.rwth-aachen.de).